

DOE/PC/92548--T12

**Suppression of Fine Ash Formation in Pulverized
Coal Flames**

DOE Grant No. DE-FG22-92PC92548

Period of Performance: September 30, 1992 to January 31, 1996

Quarterly Technical Progress Report No. 11

Period Covered by Report: April 1, 1995 to June 30, 1995

Prepared by:

JOHN C. KRAMLICH
BLAKE CHENEVERT
JUNGSUNG PARK

*Department of Mechanical Engineering
Box 352600
University of Washington
Seattle, Washington 98195-2600*

Prepared for:

DOCUMENT CONTROL CENTER

*U. S. Department of Energy
Pittsburgh Energy Technology Center
P. O. Box 10940, MS 921-118
Pittsburgh, Pennsylvania 15236-0940*

RECEIVED
USDOE/PC
95 AUG -7 PM 1:05
ACQUISITION & ASSISTANCE DIV

MASTER

Date Submitted: August 2, 1995

“U.S./DOE Patent Clearance is not required prior to the publication of this document.”

DISTRIBUTION OF THIS DOCUMENT IS UNLIMITED

DISCLAIMER

This report was prepared as an account of work sponsored by an agency of the United States Government. Neither the United States Government nor any agency thereof, nor any of their employees, makes any warranty, express or implied, or assumes any legal liability or responsibility for the accuracy, completeness, or usefulness of any information, apparatus, product, or process disclosed, or represents that its use would not infringe privately owned rights. Reference herein to any specific commercial product, process, or service by trade name, trademark, manufacturer, or otherwise does not necessarily constitute or imply its endorsement, recommendation, or favoring by the United States Government or any agency thereof. The views and opinions of authors expressed herein do not necessarily state or reflect those of the United States Government or any agency thereof.

DISCLAIMER

**Portions of this document may be illegible
in electronic image products. Images are
produced from the best available original
document.**

Introduction

One of the major obstacles to the economical use of coal is managing the behavior of its mineral matter. Ash size and composition are of critical importance for a variety of reasons. Fly ash size and emissivity affect radiant furnace heat transfer.¹ Heat transfer is also affected by the tendency of ash to adhere to heat transfer surfaces,² and the properties of these deposits.³ Removal of ash from flue gas by electrostatic precipitators is influenced by both particle size and particle resistivity.⁴ The efficiency of fabric filter-based cleaning devices is also influenced by ash size.⁵ Both types of devices have reduced collection efficiencies for smaller-sized particles, which corresponds to the size most efficiently retained in the alveolar region of the human lung.⁶ This special concern for finer sized particles has led to PM10 regulations in the last several years (PM10: particles of diameter less than 10 μm).

Laboratory work and studies of full-scale coal-fired boilers have identified two general mechanisms for ash production. The vast majority of the ash is formed from mineral matter that coalesces as the char burns, yielding particles that are normally larger than 0.5 μm . Flagen and Friedlander⁷ proposed a simple model for this residual ash, called the breakup model. In this model, each particle is assumed to yield its mineral matter as a certain specified number of ash particles (usually in the range of 1-5). This latter value is termed the "breakup number." In this way, a known pulverized coal size distribution can be transformed into a projected ash size distribution. The presumed mechanism is that each char particle fragments during combustion, carrying mineral matter with it. The major assumptions used in the model include: (1) all coal particles contain the same percentage of mineral matter, independently of size, (2) all coal particles break into exactly the same number of char particles during combustion, (3) each char particle contains the same amount of mineral matter as the other char particles, and (4) no further fragmentation occurs, which means that each offspring char particle yields its mineral matter as a single ash particle. The breakup number has been identified in recent work as being influenced by the breakup of the char during burnout, from shedding at the burning char surface,⁸ and from the fragmentation of discrete included and excluded minerals.^{9,10} Recent experimental work¹¹ and elegant site percolation modeling¹² indicate that char macroporosity is the single most important factor governing char breakup and residual ash size. Despite the severity of the assumptions, the basic breakup model has proven to be a useful engineering and interpretative tool.¹³

The second major mechanism is the generation of a submicron aerosol through a vaporization/condensation mechanism. When the ash size distribution is plotted in terms of number density, the submicron mode generally peaks at about 0.1 μm .⁴ When plotted in terms of mass, this mode is sometimes distinct from the residual ash mode,¹³ and sometimes merged into it.¹⁴ During diffusion-limited char combustion, the interior of the particle becomes hot and fuel-rich. The non-volatile oxides (e.g., Al_2O_3 , SiO_2 , MgO , CaO , Fe_2O_3) can be reduced to more volatile suboxides and elements, and partially vaporized.¹⁵⁻¹⁷ These reoxidize while passing through the boundary layer surrounding the char particle, thus becoming so highly supersaturated that rapid homogeneous nucleation occurs. This high nuclei concentration in the boundary layer promotes more extensive coagulation than would occur if the nuclei were uniformly distributed across the flow field.¹⁸ The vaporization can be accelerated by the overshoot of the char temperature beyond the local gas temperature.¹⁹

Although these particles represent a relatively small fraction of the mass, they can present a large fraction of the surface area. Thus, they are a preferred site for the condensation of the more volatile oxides later in the furnace. This leads to a layering effect in which the refractory oxides are concentrated at the particle core and the more volatile oxides reside at the surface.²⁰ This also explains the enrichment of the aerosol by volatile oxides that has been noted in samples from practical furnaces.²¹ These volatile metal oxides include the majority of the toxic metal contaminants, e.g., mercury, arsenic, selenium and nickel. Risk assessment studies suggest that toxic metal emissions represent a significant portion of the health risk associated with combustion

systems.²²

Previous work has shown that pulverized bituminous coals that were treated by coal cleaning (via froth flotation) or aerodynamic sizing exhibited altered aerosol emission characteristics. Specifically, the emissions of aerosol for the cleaned and sized coals increased by as much as one order of magnitude. At least three mechanisms have been proposed to account for this behavior.

Objectives

The goals of the present program are to:

1. Perform measurements on carefully characterized coals to identify the means by which the coal treatment increases aerosol yields.
2. Investigate means by which coal cleaning can be done in a way that will not increase aerosol yields.
3. Identify whether this mechanism can be used to reduce aerosol yields from systems burning straight coal.

Current Activities

The current experimental series focuses on the use of artificial char to study sodium vaporization and aerosol formation associated with dispersed sodium and mineral inclusions. Artificial char has the advantage over natural coal in that the composition can be precisely controlled, such that the influences of specific mineral composition and content can be investigated.

Artificial char was manufactured using the sucrose pyrolysis technique.²³ The base composition was formed by adding 0.5 grams of sodium oxalate ($Na_2C_2O_4$) to a 50 gram sucrose / 50 gram carbon black solution / suspension in distilled water. Sodium oxalate was chosen as a sodium source because of its solubility in sucrose solutions, and its low decomposition temperature (250-270°C). Sized pyrite, bentonite and calcite were added in selected quantities to produce a matrix of chars. One batch of 75 grams sucrose / 25 grams carbon / 0.5 grams sodium oxalate was also prepared to evaluate the effect of porosity on aerosol formation. The chars produced are shown in Table 1.

The solution was devolatilized at 600°C in a nitrogen environment. A ball mill was used to pulverize the resulting char into particles on the order of 40 μm diameter.

The chars were burned in the down-fired furnace described in previous progress reports. Free oxygen in the post-flame gas was set at 7.0% by volume, with the main burner operating at 66,000 Btu/hr. Residence time was about 1.4 seconds. The average temperature measured down the center of the furnace was 1100°C, as estimated by a type K thermocouple with no radiation correction. A portion of the residual ash was collected in an Andersen cascade impactor, as described in previous progress reports.

Figures 1 and 2 show the results from the calcite series. Particles that are larger than the nominal size of the first impactor stage are retained by the preseparator. These large particles are predominantly made up of unburned char. The data suggest a very high level of char burnout (of the order of 99%). Because of the large mass of carbon relative to the minerals in the starting char, the relatively high burnout still leaves the preseparator stage containing 30-40% of the collected mass. In this case, the additional mass due to the added mineral appears to be collected entirely by the preseparator stage. As shown in Figure 1, the addition of the calcite to the artificial char had

little effect on the loading on any of the impactor stages, with the exception of the preseparator. This indicates that the relatively large calcite particles (15-17 μm) do not fragment during char burnout.

Figure 2 shows that the addition of the calcite has essentially no effect on the aerosol yield. The calcite undergoes calcination to CaO at about 900°C, and the melting point of CaO is 2580°C. This suggests that the crystalline form of CaO would not exhibit much mobility at normal char combustion temperatures. Thus, it is likely that CaO would not effectively complex sodium, even if an increased surface area were made available by the use of smaller calcite particles.

Figure 3 shows the size distribution of the ash from pyrite series A. For the preseparator and the impactor stages, the general trend of Figure 3 is that increased amounts of pyrite lead to increased residual ash formation. This is not unexpected since pyrite has a relatively high melting point (1171°C), and thus would not be expected to have enough volatility to undergo significant vaporization. Thus, most of the pyrite would be expected to be found in the preseparator and on the impactor stages rather than on the backup filter.

Note in Figure 3 that the loading on the preseparator and on the impactor stages correlates with the amount of pyrite added to the char. Interestingly, the added mass appears as a proportional increase in all the stages (except the filter stage), rather than only in the preseparator. Given the relatively large size of the raw pyrite particles (9-10 μm), it would be expected that all the additional mass be found on the preseparator and on stage zero, just as it was for the calcite series shown in Figure 1. Pyrite is, however, known to fragment during char combustion, and the degree of fragmentation and its mechanism continue to be a research topic elsewhere.

In spite of the increase in mineral content, the yield of aerosol on the backup filter does not correlate with the amount of added minerals. Figure 4 shows the mass recovered at the filter stage against the amount of pyrite added to the chars. This can be taken as an indication of the aerosol yield. The results do not suggest any consistent change in sodium vaporization as the pyrite loading on the char is increased. Note that although the initial size of the pyrite particles was relatively large (9-10 μm), the size following fragmentation was similar to the original size for the bentonite, discussed below. Thus, in spite of the fact that the final size of the pyrite was small, and the surface to volume ratio was similar to the bentonite, no apparent interaction between the sodium and the pyrite was noted.

Figure 5 shows the size distribution of the ash from the bentonite experiments. It is interesting to note that although the raw bentonite particles were much smaller than the raw pyrite particles, the size distribution of the residual ash for the two were similar. The added bentonite appears as both an increase in the preseparator stage and in each of the aerodynamic impactor stages. This supports the notion that the pyrite was strongly fragmented during char combustion.

Figure 6 shows the filter yield (*i.e.*, the aerosol fraction) as a function of the amount of bentonite in the chars. The general trend is for reduced aerosol yields as the amount of bentonite increases. This suggests that the bentonite was effective at complexing sodium and reducing its overall vaporization.

Future Work

The remaining period on the current contract will be devoted to further artificial char experimentation. Model development has been suspended until after the current test series has concluded.

References

1. Gupta, R. J. Radiative Transfer Due to Fly Ash in Coal Fired Furnaces, Ph.D. Dissertation 1983, University of Newcastle.
2. Walsh, P. M., Sayre, A. N., Loehden, D. O., Monroe, L. S., Beér, J. M., and Sarofim, A. F. *Prog. Energy Combust. Sci.* 1990, 16, 327.
3. Field, M. A., Gill, D. W., Morgan, B. B., and Hawksley, P. G. W. *Combustion of Pulverized Coal.* 1967, The British Coal Utilization Research Association.
4. McCain, J. D., Gooch J. P., and Smith, W. B. *Journal of the Air Pollution Control Association* 1975, 25, 117.
5. Friedlander, S. K. *Smoke, Dust and Haze* 1977, Wiley.
6. Morrow, P. E. *Amer. Ind. Hyg. Assoc. J.* 1964, 25, 213.
7. Flagen, R. C., and Friedlander, S. K. *Recent Developments in Aerosol Science.* (D. T. Shaw, Ed.) 1978, Wiley, Chapter 2.
8. Helble, J. J., and Sarofim, A. F. *Combust. Flame* 1989, 76, 183.
9. Baxter, L. L. *Prog. Energy Combust. Sci.* 1990, 16, 261.
10. Srinivasachar, S., Helble, J. J., and Boni, A. A. *Prog. Energy Combust. Sci.* 1990, 16, 281.
11. Helble, J. J., and Sarofim, A. F. *Combust. Flame* 1989, 76, 183.
12. Kang, S., Helble J. J., Sarofim A. F., and Beér, J. M. *Twenty-Second Symposium (International) on Combustion* 1988, The Combustion Institute, p. 231.
13. Flagen, R. C. *Seventeenth Symposium (International) on Combustion* 1979, The Combustion Institute, p. 97.
14. Linak, W. P., and Peterson, T. W. *Aerosol Sci. Technol.* 1984, 3, 77.
15. Neville, M., Quann, R. J., Haynes, B. S., and Sarofim, A. F. *Eighteenth Symposium (International) on Combustion* 1981, The Combustion Institute, p. 1267.
16. Senior, C. L., and Flagen, R. C. *Aerosol. Sci. Technol.* 1982, 1, 371.
17. Quann, R. J., and Sarofim, A. F. *Nineteenth Symposium (International) on Combustion* 1982, The Combustion Institute, p. 1429.
18. Damle, A. S., Ensor, D. S., and Ranade, M. B. *Aerosol Sci. Technol.* 1982, 1, 119.
19. Quann, R., Neville, J. M., and Sarofim A. F. *Combust. Sci. Technol.* 1990, 74, 245.
20. Gladney, E. S., Small, J. A., Gordon, G. E., and Zoller, W. H. *Atmos. Environ.* 1976, 10, 1071.
21. Linak, W. P., and Peterson, T. W. *Twenty-First Symposium (International) on Combustion* 1986, The Combustion Institute, p. 399.
22. Smith, A. H., and Goeden, H. M. *Combust. Sci. Technol.* 1990, 74, 51.
23. Helble, J. J., Ph.D. Dissertation, Department of Chemical Engineering, Massachusetts Institute of Technology, Cambridge, MA (1987).

Char Batch	Dry Mass in Grams Prior to Pyrolysis (Form of Component)					
	Sucrose (in solution)	Carbon Black (40-60 nm)	Sodium Oxalate (in solution)	Pyrite (9-10 μm)	Bentonite (0.9 -1 μm)	Calcite (15-17 μm)
A	50	50	0.5			
B	75	25	0.5			
C	50	50	0.5	0.925		
D	50	50	0.5	1.850		
E	50	50	0.5	2.775		
F	50	50	0.5	3.700		
G	50	50	0.5		1.25	
H	50	50	0.5		2.50	
I	50	50	0.5		3.75	
J	50	50	0.5		5.00	
K	50	50	0.5			0.25
L	50	50	0.5			0.50
M	50	50	0.5			0.75
N	50	50	0.5			1.00

Table 1. Char composition matrix

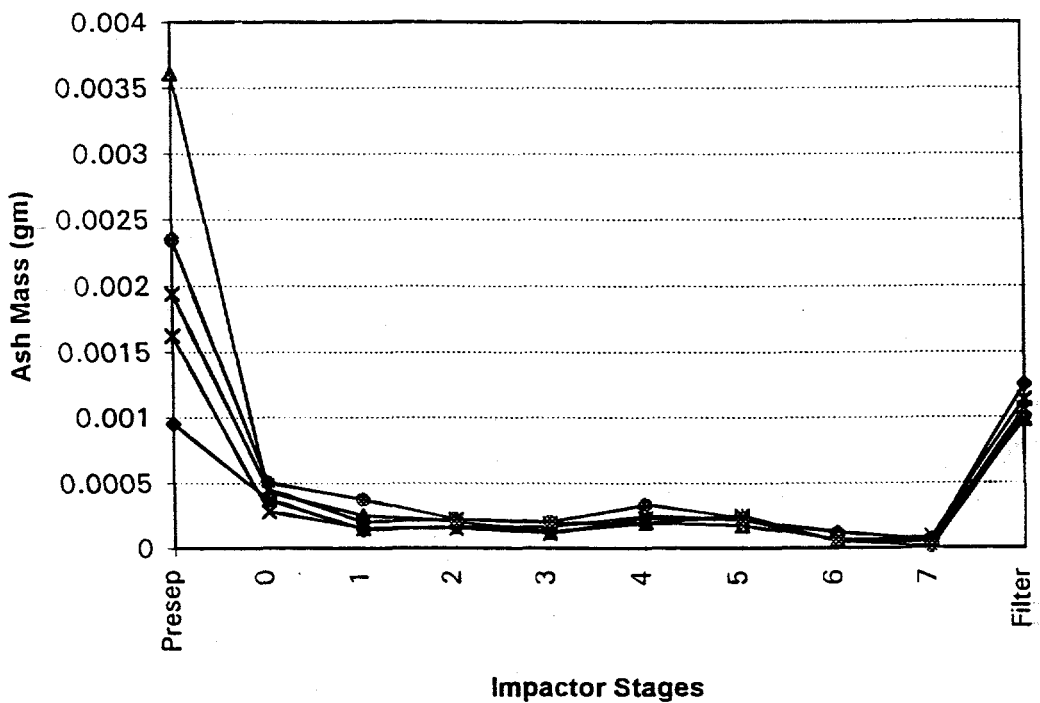


Figure 1. Impactor stage yields for the calcite series: (◆ - char A; △ - char K, ✗ - char L, ★ - char M, ○ - char N).

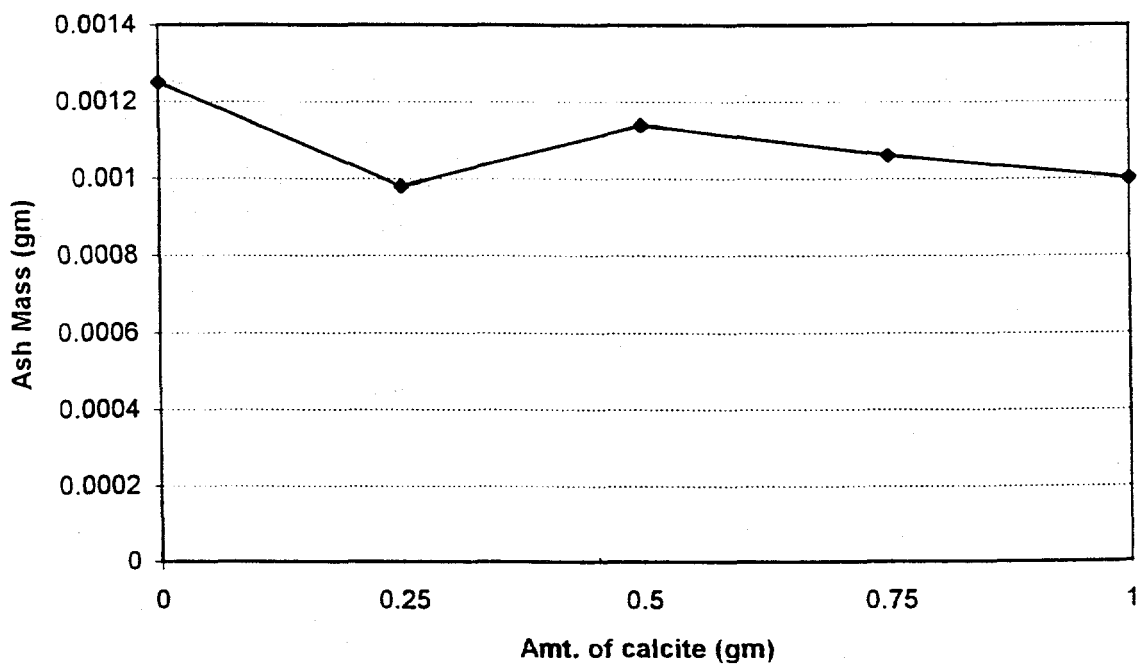


Figure 2. Ash yield at the filter vs. amount of calcite for calcite series.

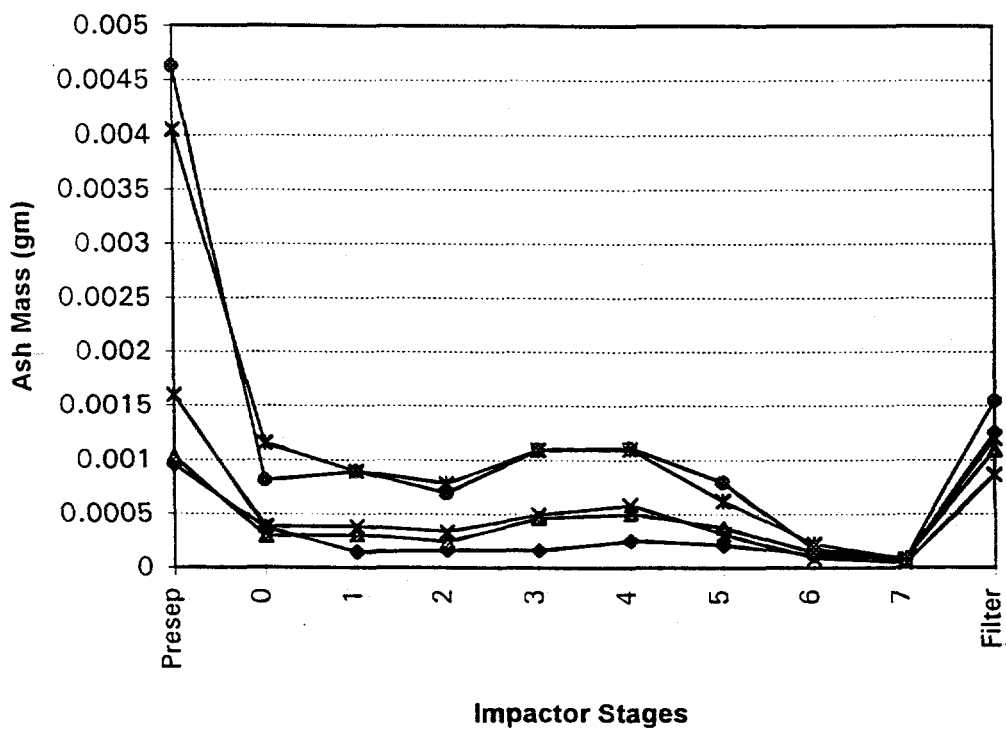


Figure 3. Impactor stage yields for the pyrite series: (◆ - char A; △ - char C, ✕ - char D, * - char E, ○ - char F).

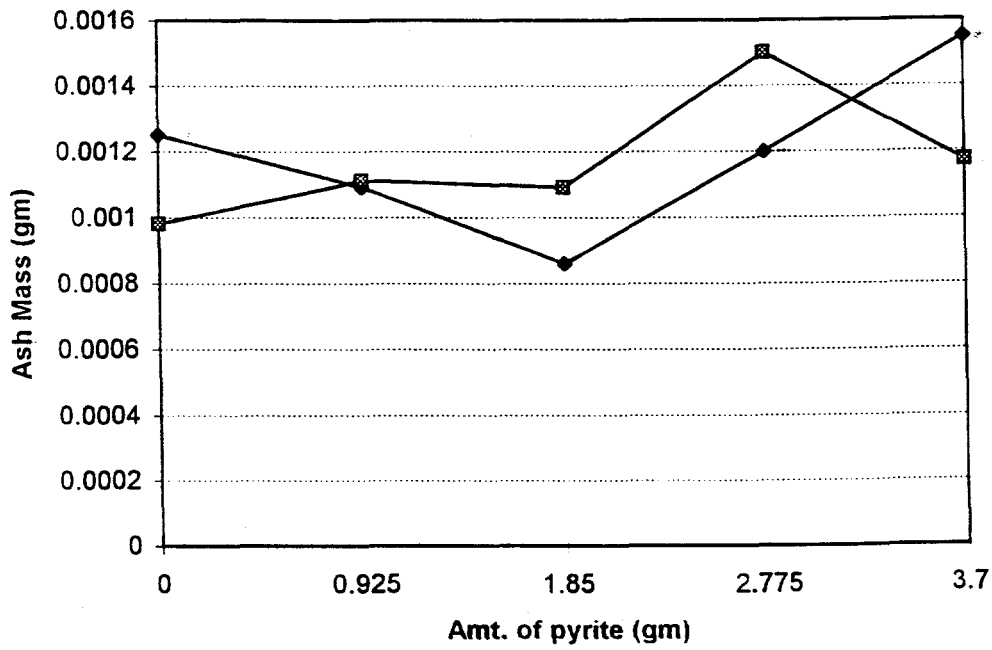


Figure 4. Aerosol yield vs. amount of pyrite in the char for two separate pyrite series.

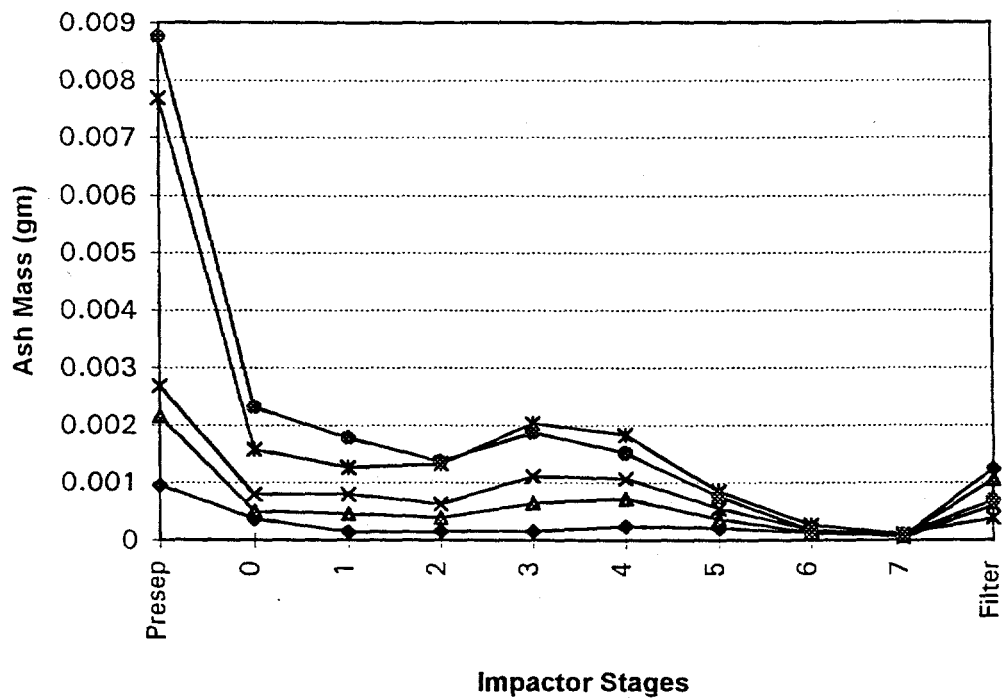


Figure 5. Impactor stage yields for the bentonite series: (◆ - char A; △ - char G, ✗ - char H, ★ - char I, ○ - char J).

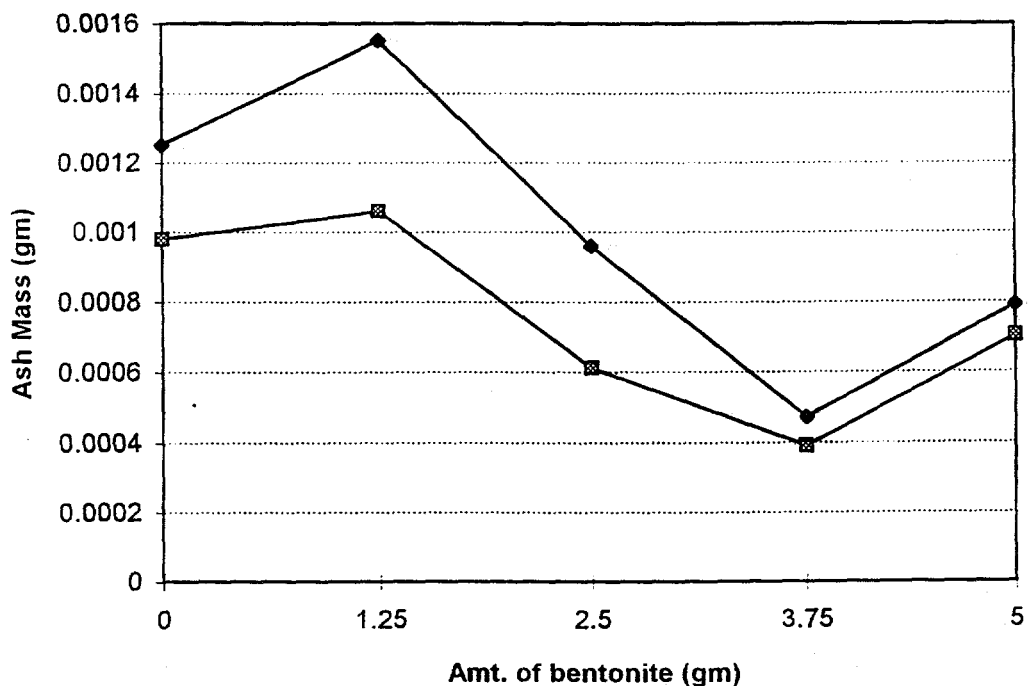


Figure 6. Aerosol yield vs. amount of bentonite in the char for two separate bentonite series.